

Processing Techniques for the 93 K Superconductor $\text{Ba}_2\text{YCu}_3\text{O}_7$

D. W. MURPHY, D. W. JOHNSON, JR., S. JIN, R. E. HOWARD

Superconductivity above the temperature of liquid nitrogen in copper oxide-based systems has led to optimism that superconductors may at last find wide application. The critical temperature, however, is just one of the required parameters. The materials must be made into usable forms such as wire, thick films, thin films, and bulk ceramics. In addition, the critical current in these various forms is a crucial test of their utility. This article reviews the processing techniques used to fabricate potentially useful forms and assesses remaining problems. Considerable improvement in critical current density is necessary in bulk materials, and thin films need to be made compatible with other thin-film technology.

THE DISCOVERY OF SUPERCONDUCTIVITY IN COPPER oxide-based ternary and quaternary systems by J. G. Bednorz and K. A. Müller (1) has led to superconductivity at unprecedented high temperatures and rekindled a long-standing hope that superconductors might form the basis of a new age of technology. As remarkable as the advances have been, considerable improvement in many areas will be required before the new superconductors affect commercial technology. As is the case for any technology based on materials, one of the most crucial areas is high quality synthesis and processing. The popular press has suggested that the new superconductors are so easy to make that a high school student with a few chemicals and a microwave oven can easily prepare them. Indeed, much of the enthusiasm and progress in the field has been the result of the relatively easy synthesis of material that exhibits zero resistance and some magnetic flux exclusion above liquid nitrogen temperature (77 K). However, the preparation of material with high critical currents and in forms, such as wires and thin films on semiconductors, that are suitable for applications remains a formidable challenge.

To date there are four main classes of high transition temperature (T_c) copper oxide superconductors, designated by La_2CuO_4 ($T_c = 40$ K) (1-3), $\text{Ba}_2\text{YCu}_3\text{O}_7$ ($T_c = 93$ K) (4-5), Bi-Sr-Ca-Cu-O ($T_c = 80$ to 110 K) (6), and Tl-Ba-Ca-Cu-O ($T_c = 80$ to 125 K) (7, 8). In this article we present an overview of processing techniques for $\text{Ba}_2(\text{RE})\text{Cu}_3\text{O}_{7-x}$ (RE = La, Y, Nd, Sm, Eu, Gd, Dy, Ho, Er, Tm, Yb, Lu), concentrating on $\text{Ba}_2\text{YCu}_3\text{O}_7$ as a prototype. Although this material is popularly known as "1-2-3" on the basis of the formula $\text{Y}_1\text{Ba}_2\text{Cu}_3\text{O}_7$, we use the accepted chemical nomenclature, $\text{Ba}_2\text{YCu}_3\text{O}_7$. We review $\text{Ba}_2\text{YCu}_3\text{O}_7$ here because it has been

the most thoroughly studied of these materials to date. Processing of the other classes of high T_c copper oxide systems shares many of the general features described here, but there are also important differences between each of the classes.

The superconducting $\text{Ba}_2(\text{RE})\text{Cu}_3\text{O}_{7-x}$ phases have been prepared in many forms including polycrystalline powders, single crystals, ceramic objects, composites, wires, and thin films. Several of these forms and the methods used to prepare them will be described in this article, but several other very promising approaches will not be included for lack of space. With over 3000 papers published in a single year it is impossible for this account to be comprehensive. Before discussing the processing, some of the fundamental superconducting properties and materials chemistry important to all the processing methods are outlined.

Superconducting Properties of $\text{Ba}_2\text{YCu}_3\text{O}_7$

There is no generally accepted microscopic theory that explains the occurrence of superconductivity in these materials. Phenomenologically, however, once the cuprates become superconducting they behave like other type II superconductors and Ginzburg-Landau theory is applicable (9). Some relevant parameters for $\text{Ba}_2\text{YCu}_3\text{O}_7$ are compared with those of Nb_3Sn in Table 1. Both the T_c and the critical magnetic field (H_{c2}) are high, as required for many applications.

The critical current density (J_c), is also a crucial parameter for applications, but is not listed in Table 1 because it is not an intrinsic property and is strongly affected by structural features (defects, grain boundaries, impurities, and so forth) on the scale of both the coherence length (ξ) and the penetration depth (λ). Structural

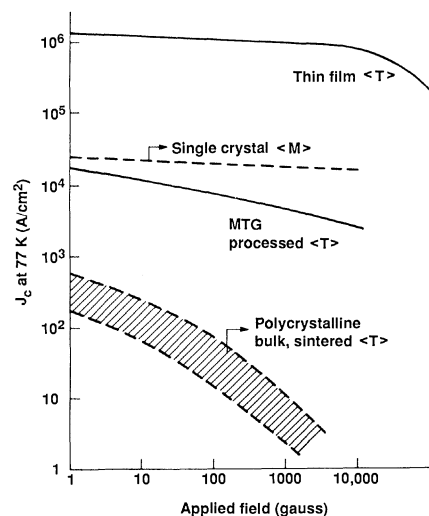


Fig. 1. The critical superconducting current density J_c as a function of applied magnetic field at 77 K for different forms of $\text{Ba}_2\text{YCu}_3\text{O}_7$ discussed in this article, as measured by transport (<T>) or magnetically (<M>). The data on crystals are from (14).

D. W. Murphy, D. W. Johnson, Jr., and S. Jin are at AT&T Bell Laboratories, 600 Mountain Avenue, Murray Hill, NJ 07974. R. E. Howard is at AT&T Bell Laboratories, Crawfords Corner Road, Holmdel, NJ 07733.

Table 1. Comparison of superconducting properties of $\text{Ba}_2\text{YCu}_3\text{O}_7$ and Nb_3Sn . Symbols (\perp) and (\parallel) refer to values perpendicular and parallel to the a - b plane, respectively. Temperatures at which critical fields were measured are in parentheses.

Material	T_c (K)	H_{c2} (T)	Coherence length ξ (Å)	Penetration length λ (Å)
Nb_3Sn	18	22 (4.2 K)	20 to 30	400
$\text{Ba}_2\text{YCu}_3\text{O}_7$	93	6 (\perp), 60 (\parallel) (77 K) 100 (\perp) (30 K)	2 to 15	1500

features on the order of ξ can lead to pinning centers beneficial to J_c , but control is necessary to avoid large regions that do not superconduct. Little is known about pinning centers in $\text{Ba}_2\text{YCu}_3\text{O}_7$, but ξ is extremely short and anisotropic in this material (10–13). Values of ξ as small as 2 Å (12) have been reported, suggesting that even single atom defects could be important.

Different forms of $\text{Ba}_2\text{YCu}_3\text{O}_7$ have different critical currents (Fig. 1). Each of these forms will be described in more detail later, but it is important to point out here the widely varying values of J_c and the dependence of J_c on field. Oriented thin films have been made with $J_c \approx 4 \times 10^6$ A/cm² (measured at 77 K at zero field) (15, 16) whereas for bulk, sintered ceramics J_c is generally less than 1000 A/cm². Because most applications require operation in high magnetic fields, the dependence of J_c on field is crucial. At 77 K, transport measurements of J_c show a decrease with applied field. Furthermore, the lower the zero-field J_c , the more rapid the decrease. The rapid drop in J_c with field is typical of “weak link” superconductors and arises from tunneling of the supercurrent between isolated regions of superconductivity separated by a thin, nonsuperconducting barrier. Many of the large-scale applications of superconductivity require large currents at high fields as shown in Fig. 2. Also shown in Fig. 2 are the present capabilities of Nb-Ti and Nb_3Sn wires at 4.2 K ($T/T_c = 0.45$ and 0.23, respectively) compared to extrapolated behavior of the best bulk $\text{Ba}_2\text{YCu}_3\text{O}_7$ at 77 K ($T/T_c = 0.85$). At a comparable T/T_c (20 K, $T/T_c = 0.21$) $\text{Ba}_2\text{YCu}_3\text{O}_7$ thin films can carry more than 5×10^5 A/cm² at 15 T (17), which is significantly better than Nb_3Sn at 4.2 K (18). However, equivalent behavior at 77 K will require a much higher T_c .

Materials Chemistry

Structure. Several different levels of structure are important to superconductivity, ranging from the ideal crystallographic structure to defects and the nature of grain boundaries. The crystal structures of $\text{Ba}_2\text{YCu}_3\text{O}_7$ and many of its substitutional analogs have been determined by both x-ray (19) and neutron diffraction (20–23). The structure is a defect (O atoms) perovskite superstructure (resulting from ordering of Y and Ba). The oxygen ordering results in the coexistence of both two-dimensional $[\text{CuO}_2]_\infty$ layers and $[\text{CuO}_3]_\infty$ chains. The two-dimensional $[\text{CuO}_2]_\infty$ layers are common to all of the known copper oxide superconductors. The presence of layers and chains makes the structure highly anisotropic. Anisotropy is evident in transport properties (24) such as the normal state conductivity, as well as H_{c2} and J_c in the superconducting state (25). The anisotropy in the conductivity just above T_c measured on single crystals is ≈ 100 with the highest conductivity in the plane of the layers. Anisotropy attributable to the chains has not been measured because twinning (26–28) along the $[110]$ direction interconverts the chain direction between twins. Twinning is an example of a structural defect that may be important to superconductivity be-

cause it occurs on the size scale of ξ . Several other types of defects such as extra layers and anti-phase boundaries have also been observed.

Phase equilibria. A detailed phase diagram is an invaluable guide to materials synthesis. It is of course possible and often important to prepare materials that are not thermodynamically stable (such as a thin film stabilized by epitaxy or strain), but knowledge of the phase diagram is an excellent guide even in these cases. Even though superconductivity can be observed when only a small portion of the sample is superconducting, it is critical that phase-pure material be used for meaningful scientific measurements and for most practical applications.

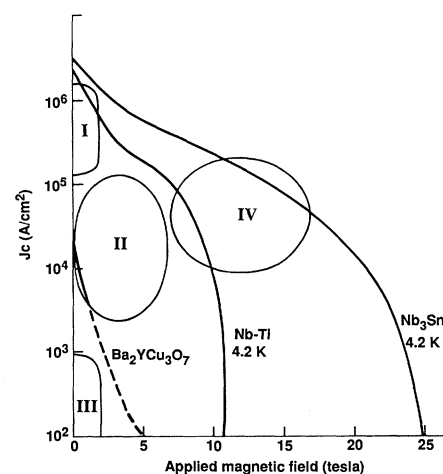
When superconductivity was discovered in the Y-Ba-Cu-O system, the only previously known compound that contained each of these elements was BaY_2CuO_5 (29), a green, insulating material. The superconducting phase was quickly identified as $\text{Ba}_2\text{YCu}_3\text{O}_{7-x}$ (5). Several preliminary phase diagrams have now been published (30–32) and are in general agreement. The diagram in Fig. 3 represents an isothermal cut at 950° to 1000°C in air. The amount of oxygen in each phase is fixed by the ambient. Two of the salient features of the phase diagram are the narrow compositional range of the superconducting phase in Y, Ba, and Cu and the region of partial melting. Phase diagrams have not been determined for other rare earths, but there are indications that most are similar, for example, $\text{Ba}(\text{RE})_2\text{CuO}_5$ (29) and $\text{Ba}_2(\text{RE})\text{Cu}_3\text{O}_7$ (33–35) compounds exist for most rare earths. However, the larger rare earths have a wider stability range for $\text{Ba}_{2-y}(\text{RE})_{1+y}\text{Cu}_3\text{O}_x$ ($0 < y < 0.5$) (36).

Single crystals as large as 1 cm \times 1 cm \times 200 μm have been grown from the region of partial melting close to $\text{Ba}_2\text{YCu}_3\text{O}_7$ (37–39). Numerous physical property measurements on these crystals have formed the basis for much of our understanding of these materials.

Substitutions on the Cu sites by Al, Ni, Fe, Co, Zn, and other metals have been reported (40–43). In contrast to substitutions for Y, these all lead to marked decreases in T_c .

The role of oxygen stoichiometry. A remarkable feature of $\text{Ba}_2\text{YCu}_3\text{O}_x$ is that the stoichiometry in oxygen is readily variable over the range $6.0 \leq x \leq 7.0$ (44–48). The stoichiometry as a function of temperature and ambient are shown in Fig. 4. The effect of oxygen stoichiometry on the electronic properties is dramatic. At $x \approx 7.0$ the superconducting T_c is maximized and for $x \approx 6.0$ the material is a semiconductor. The structure at $x = 6$ is related to that at $x = 7$ by the total absence of the oxygen atoms connecting copper atoms along the chains (49, 50). The activation energy for oxygen diffusion has been estimated at 1.1 eV (47, 48, 51), and the kinetics are slow at room temperature, allowing stability of samples over the entire

Fig. 2. Required current-field domains for various superconducting devices such as high-current interconnects (I); magnetic-resonance imaging magnets (II); superconducting quantum interference devices (III); and magnets for the Superconducting Supercollider (IV). Also shown are the capabilities of currently available Nb-Ti and Nb-Sn superconducting wire at 4.2 K and projected values for $\text{Ba}_2\text{YCu}_3\text{O}_7$ based on the MTG current density shown in Fig. 1 (18).



range $6.0 \leq x \leq 7.0$. Materials prepared or sintered in excess of 900°C have $x \approx 6.3$ and must be annealed at 400° to 500°C in oxygen to obtain the highest oxygen content and T_c . Films, powders, and porous ceramic samples readily equilibrate with oxygen at 400° to 500°C , but dense ceramics and large single crystals require longer times, increasing as the square of the distance over which oxygen must diffuse.

The structural and electronic properties at intermediate oxygen stoichiometry are dependent on the conditions of preparation in addition to the total oxygen stoichiometry. Quenching from high temperature maintains the tetragonal structure for $x < 6.6$ (52), whereas removal of oxygen at low temperatures maintains the orthorhombic structure at least to $x = 6.3$ (53). A T_c of 60 K is obtained for materials in which oxygen is removed at low temperatures by gettering (53) or by vacuum annealing (54). Several studies indicate that the oxygen in these intermediate T_c samples is ordered to give superstructures (55–57). It is fortunate that the optimum superconducting properties in this system are attained with a relatively simple anneal.

Chemical reactivity. In addition to the reversible reaction with oxygen, $\text{Ba}_2\text{YCu}_3\text{O}_7$ is degraded by reaction with atmospheric H_2O and CO_2 . The reaction with H_2O liberates O_2 and leads to formation of $\text{Ba}(\text{OH})_2$, Y_2BaCuO_5 , and CuO (58–60). The rate of deterioration in liquid or atmospheric H_2O is strongly dependent on temperature and surface area. In most forms, $\text{Ba}_2\text{YCu}_3\text{O}_7$ may be handled in air without significant changes in properties, but long-term stability will require protection. The stability of BaCO_3 is a strong driving force for the reaction of $\text{Ba}_2\text{YCu}_3\text{O}_7$ with CO_2 . Carbon at grain boundaries (61) (most likely as a carbonate) has been implicated in ceramic material and may contribute to the weak-link behavior. The effects of both H_2O and CO_2 may be reversed at high temperature.

At synthesis temperatures (800° to 950°C) $\text{Ba}_2\text{YCu}_3\text{O}_7$ is reactive toward most common ceramic or metallic crucible materials and potential thin-film substrate materials. The only materials we have found to be inert are silver and, to a lesser extent, gold. The reactivity toward crucible materials increases with temperature and extent of contact. For shaped ceramics it is best to place the object on a bed of powder of the same composition. For thin-film processing, reactivity with substrates is a severe problem because of the intimate contact and short diffusion distances. This greatly restricts the choice of substrates and mandates the shortest possible processing times at the lowest possible temperatures.

Processing of Bulk Materials

Processing methods common to ceramic technologies have been used to synthesize and form $\text{Ba}_2\text{YCu}_3\text{O}_7$ into bulk shapes. This is accomplished by first shaping an assemblage of particles and then densifying them into a solid part by sintering at high temperature. The driving force for densification is the reduction of the excess free energy associated with the surfaces of the particles. Therefore, ceramic materials are generally processed from finely divided powders to maximize this surface free energy.

Processing of bulk objects can be subdivided into the steps of powder preparation, forming, and sintering. These will be addressed in turn for $\text{Ba}_2\text{YCu}_3\text{O}_7$. We will then discuss the technologically important areas of wire processing and methods for increasing J_c .

Powder preparation. Conventional ceramic powder preparation methods may be used for $\text{Ba}_2\text{YCu}_3\text{O}_7$. Generally, this consists of mixing the appropriate ratios of the constituent oxides or oxide precursors such as carbonates or nitrates. For $\text{Ba}_2\text{YCu}_3\text{O}_7$, typical starting materials are BaCO_3 , Y_2O_3 , and CuO . For small batches

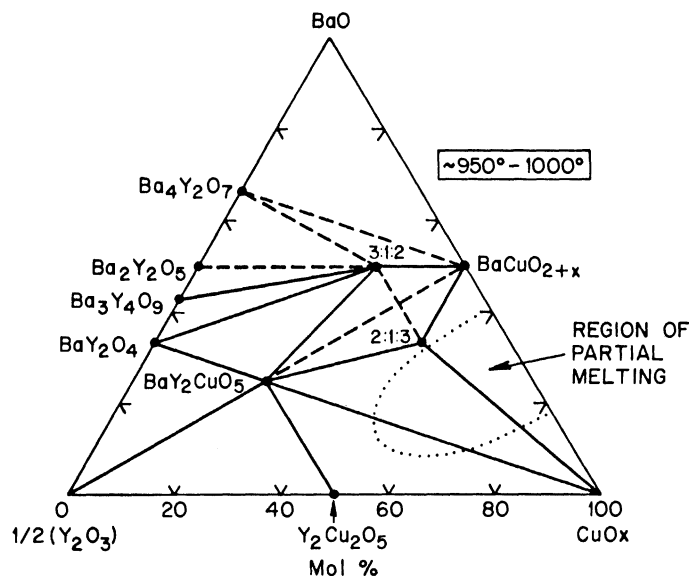
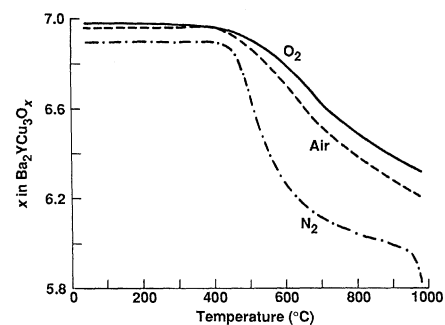


Fig. 3. The Ba-Y-Cu-O phase diagram for materials prepared at 950° to 1000°C in air (30).

Fig. 4. The oxygen stoichiometry as a function of temperature in O_2 , air, and N_2 obtained by thermogravimetry. Weight changes are reversible in O_2 and air (44).



(<100 g) these can be mixed dry by means of laboratory devices such as a mortar and pestle. For larger batches, they are mixed in a water slurry with high shear mixers or ball mills, filtered, dried, and heat treated (calcined) at 875° to 925°C . The calcination step serves to decompose the carbonate and interdiffuse the starting materials for phase formation and chemical homogenization. After calcination the material is again ground to subdivide any aggregated products and to further enhance chemical homogenization. At this point the powder can be used in the subsequent fabrication steps or recalcined for better homogeneity and phase purity. Although the raw materials suggested here successfully produce the superconducting phase, many others can be used. For instance, $\text{Ba}(\text{OH})_2$, $\text{Ba}(\text{NO}_3)_2$, BaO_2 , BaF_2 , $\text{Y}_2(\text{CO}_3)_3$, CuCO_3 , and $\text{Cu}(\text{NO}_3)_2$ can all be used as source materials. Although BaCO_3 has the advantage of having a stable composition, it is somewhat difficult to decompose at the temperatures used for calcination and thus care must be exercised in large batches to assure that the CO_2 is continually removed with either flowing air or oxygen during calcination.

A broad spectrum of other powder preparation techniques have also been applied to oxide superconductors. These include sol-gel (62–66), coprecipitation (64, 67, 68), nitrate precursors (69), and freeze drying (70). These methods have the goal of obtaining powders with high chemical homogeneity and very fine particles, which may lead to low temperature phase formation and sintering. In addition, some methods offer specific advantages for preparation of material in a particular form or batch size.

Forming. To make ceramic objects useful for experimentation or devices the $\text{Ba}_2\text{YCu}_3\text{O}_7$ powder must be formed into shapes before

sintering. The most widely used technique is dry pressing, which consists of filling a die body with powder and pressing at 50 to 500 MPa into a compacted shape. The powder can also be loaded in a sealed elastomeric enclosure and placed in a chamber under high fluid pressure to isostatically press a shape. Frequently 1 to 3% by weight of an organic binder such as polyvinyl alcohol is added to the powder to enhance the strength of the pressed part.

Addition of 10 to 20% by weight of organic binder gives a stiff paste that can be used to extrude shapes. Here, the mix is loaded into a screw or ram extruder that forces the material through a die orifice yielding a continuous part having the cross section of the die. This has been used for $\text{Ba}_2\text{YCu}_3\text{O}_7$ yielding thin, flexible, wire-shaped strands of the ceramic powder in the organic binder (7).

Screen printing uses a slurry containing powder, binder, and solvent with a consistency similar to that of toothpaste. The slurry is forced through a fine mesh patterned stainless steel screen with a rubber bar leaving a 10- to 20- μm -thick layer of the slurry on a substrate. Similar technology is used in multilayer ceramic capacitors, ceramic packages, and thick film hybrid integrated circuits. Some patterns of $\text{Ba}_2\text{YCu}_3\text{O}_7$ formed by screen printing are shown in Fig. 5. For the large plates, the substrates are presintered Al_2O_3 . Critical current densities of these screen-printed thick films at 77 K are $\leq 200 \text{ A/cm}^2$.

Tape casting uses a similar slurry with the viscosity of heavy paint. This technology is currently used to form ceramic substrates, the dielectric layers in multilayer ceramic capacitors, and the main body material for ceramic packages. The slurry is spread in an even layer over a carrier film. Evaporation of solvent leaves a tape 0.02 to 1 mm thick that can be separated from the carrier. Because this unsintered tape still contains organic binders, it is flexible and can be cut, punched, rolled, or laminated. After shaping, the tape is sintered to give good interparticle contact and is no longer flexible. Figure 6 shows unsintered tape of $\text{Ba}_2\text{YCu}_3\text{O}_7$ illustrating its flexibility and a sheet of sintered tape about 10 cm on edge and 150 μm thick. The properties of $\text{Ba}_2\text{YCu}_3\text{O}_7$ sintered from tapes are comparable to those made by dry pressing (72) with J_c on the order of 1000 A/cm^2 (73).

There are many other conventional methods of shaping ceramics, and several have been applied to high-temperature superconductors. One example is a freestanding helical shape of $\text{Ba}_2\text{YCu}_3\text{O}_7$ made by injection molding (74).

Sintering. Because $\text{Ba}_2\text{YCu}_3\text{O}_7$ melts incongruently at about 980°C, sintering by solid-state transport mechanisms is limited to the range of 900° to 975°C. An oxygen flow during sintering is used to facilitate the removal of the organic binders, to aid in the removal of CO_2 from residual carbonates, and to maximize the oxygen content of the final sintered body.

Before sintering the binder is burned off by slowly heating to 300°C. The heating rate to the sintering temperature can then be rapid, except that above 900°C a slower rate (20°C per hour) is used to facilitate decomposition of any carbonate and prevent excessive trapped porosity. Typical sintering times are several hours. After sintering, a final annealing in oxygen at 400° to 600°C maximizes incorporation of oxygen. The anneal temperature is a compromise between higher temperatures where oxygen diffusion rates are higher and lower temperatures where the thermodynamic equilibrium favors higher oxygen contents (46). The anneal time depends on the sintered density and thickness of the part. For dense ceramics with thicknesses on the order of 1 cm, the anneal time at 500°C may be 1 to 2 days.

A novel technique for forming and densifying superconducting powder in one step is explosive compaction (75). Here the powder is placed in a shaped cavity between copper plates and densified by detonation of an explosive charge. The temperature of the sample

remains low, allowing the formation of shapes without loss of oxygen.

Wire fabrication. Existing high power superconductivity applications (electromagnets) use multifilamentary composite wires containing both the superconductor and a normal metal. This design serves several important functions: (i) minimization of energy dissipation by magnetic flux instabilities, (ii) ac loss reduction, (iii) a parallel electrical conduction path to carry current in case of local loss of superconductivity, (iv) thermal stabilization (heat sinking) to minimize local heating and prevent catastrophic loss of superconductivity, and (v) mechanical protection of the superconducting core against the Lorentz force during operation and other stresses of fabrication, handling, or use. In the case of $\text{Ba}_2\text{YCu}_3\text{O}_7$, a normal metal cladding could also provide environmental protection.

Brittleness is a commonly cited problem in the fabrication of oxide superconductors, but it is also a problem with Nb_3Sn and has prevented its greater use compared to the more ductile Nb-Ti even though the former has a higher T_c and H_{c2} . In the case of Nb_3Sn , good superconducting wire with reasonable flexibility can be obtained by reaction of thin Nb wire with a Cu-Sn matrix, leaving a thin film of Nb_3Sn embedded between Nb and the Cu-Sn matrix (76).

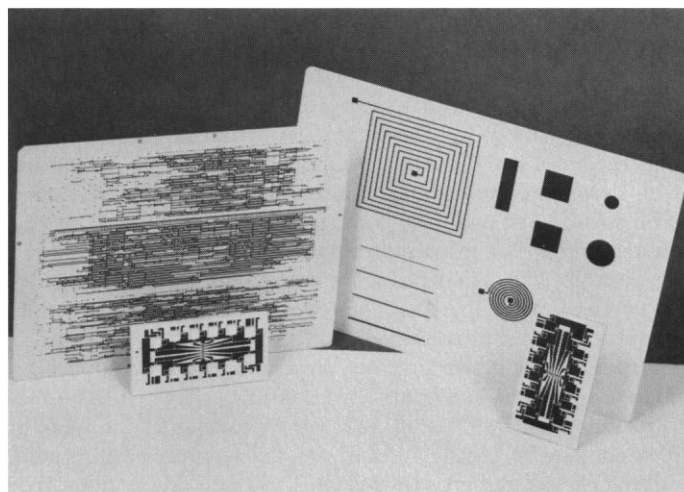


Fig. 5. Examples of screen-printed $\text{Ba}_2\text{YCu}_3\text{O}_7$ on alumina substrates.

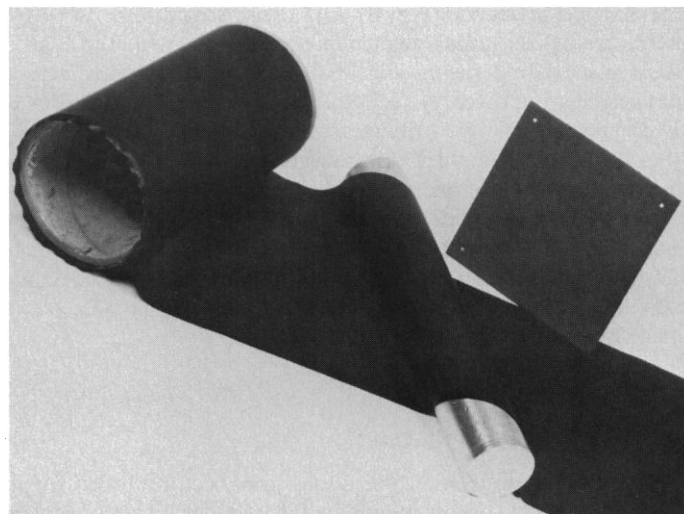


Fig. 6. A roll of tape-cast $\text{Ba}_2\text{YCu}_3\text{O}_7$ before sintering and a sintered sheet (10 cm \times 10 cm).

Several different approaches to single filament $\text{Ba}_2\text{YCu}_3\text{O}_7$ metal composite wire have been reported. One example is the drawing of a preform consisting of a nonreactive tube (such as silver or silver-coated metal) packed with finely pulverized $\text{Ba}_2\text{YCu}_3\text{O}_7$ superconductor powder (77). During drawing the superconducting powder conforms to the overall wire geometry. The final metal-clad composite wire (Fig. 7), is then wound over a mandrel into a coil geometry, sintered, and annealed. Alternatively a composite wire in which $\text{Ba}_2\text{YCu}_3\text{O}_7$ envelopes a normal metal wire core may be obtained by coating the normal wire with a $\text{Ba}_2\text{YCu}_3\text{O}_7$ slurry followed by sintering (78). This configuration does not offer environmental protection of the superconductor as does the metal-clad version, but it improves the control of oxygen stoichiometry. Wires have also been produced from melt-spun molten oxide (78) and from precursor metal alloys (79).

The extrusion method described earlier has been used to fabricate continuous, wire-like strands of $\text{Ba}_2\text{YCu}_3\text{O}_7$ (71). As extruded, the strand contains a binder that must be removed and the wire sintered to make a connected superconducting path. This approach can also use strips of the tape described earlier, which could be laminated with a normal metal. The flexible nature of the unsintered material aids in shaping the wire before sintering, but does not lead to a ductile superconducting wire.

Most of these wires have J_c less than 1000 A/cm^2 in zero field, but 2000 A/cm^2 has been reported in thin, silver clad ribbons made by wire drawing and cold rolling (80).

It is too early to predict an eventual practical wire fabrication method, but it is clear that substantial progress is required.

Processing for high J_c . The techniques described above all lead to bulk materials with J_c below $\approx 2000 \text{ A/cm}^2$ at 77 K in zero field with a rapid drop at high fields as shown in Fig. 1. These values are far too low to be useful. In contrast, measurements of J_c on single crystals and thin films demonstrate that significant improvements are possible. The field dependence is attributed to low J_c weak links (81) between high J_c grains. These weak links are generally attributed to the presence of nonsuperconducting impurities, poor mechanical connectivity between grains, structural or compositional deviation at interfaces, and crystal lattice effects.

Recent work by Jin *et al.* (82, 83) indicates that the weak link problem can be greatly reduced by a new processing technique called melt-textured-growth (MTG). Unlike the conventional method of sintering, this new technique employs partial or complete melting of $\text{Ba}_2\text{YCu}_3\text{O}_7$ followed by controlled recrystallization. The MTG technique transforms the granular, random microstructure of the sintered precursor (Fig. 8) to a dense structure consisting of long, needle-like grains aligned predominantly with the high J_c basal plane along the needle axis. This microstructure leads to dramatically improved J_c ($1.7 \times 10^4 \text{ A/cm}^2$ at 77 K and $H = 0$). Even more significant is the much reduced field dependence of J_c ($\approx 4000 \text{ A/cm}^2$ at $H = 1 \text{ T}$) as shown in Fig. 1. Although additional improvement in J_c of one to two orders of magnitude is still needed at even higher magnetic fields, these results are very encouraging, and offer hope for continued improvement in J_c of bulk materials. To date the MTG process has been used only on short laboratory samples. Its use on large pieces or long wires will be necessary to make it useful.

Thin-Film Fabrication

A variety of electronic applications have been proposed for the new superconductors including high-speed chip interconnections (84, 85) or even active devices (86, 87). Much of the excitement in this area comes from the fact that for the first time superconductivity

occurs at temperatures where it is practical to operate semiconductor devices. In fact, because of factors like mobility, thermal conductivity, and noise, liquid nitrogen temperature is almost optimal for the operation of either silicon or gallium arsenide field effect transistor (FET) circuits. In the past, superconducting electronics at liquid helium temperature required a completely new technology; now at higher temperatures the opportunity to blend incrementally with existing semiconductor electronics appears possible. Such a merger, though, will require a well-controlled superconducting thin-film technology before experiments can begin to determine where significant applications can be made. This technology must encompass a range of processing techniques including the formation of thin films (0.1 to $2.0 \mu\text{m}$), patterning and etching of the films, and interfacing them to other circuitry.

There are three main components to the formation of high quality thin films of $\text{Ba}_2\text{YCu}_3\text{O}_7$: stoichiometry, crystallinity, and substrate interaction. The first requirement is to provide the relevant atoms in a precise stoichiometric ratio. As in the bulk material, even small

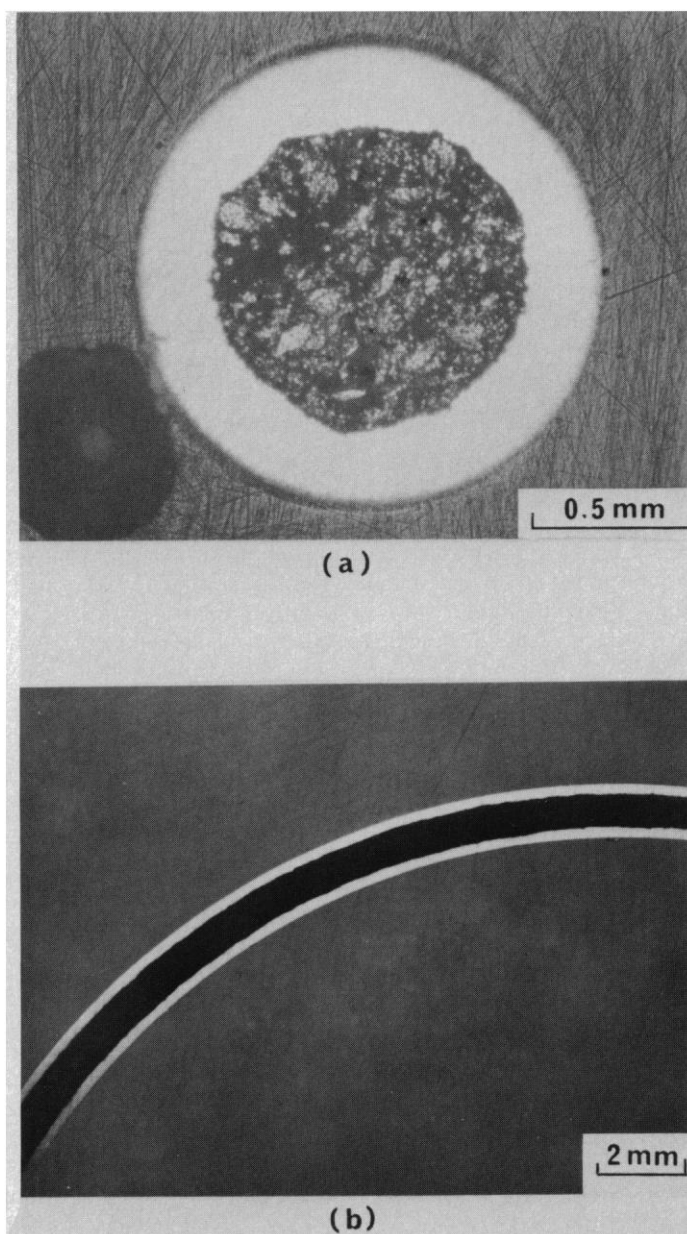


Fig. 7. Photomicrographs of $\text{Ag}/\text{Ba}_2\text{YCu}_3\text{O}_7$ composite superconductor wire in (a) cross section and (b) a longitudinal section (77).

variations in composition can result in formation of undesirable phases at the grain boundaries and result in a degradation of electrical properties. Next, the correct phase must be formed by proper heat treatment and oriented with the substrate so as to take the best advantage of the highly anisotropic current-carrying capacity (25, 88). The heat treatment may be done either during deposition or after the film is formed. The oxygen stoichiometry is controlled by the oxygen concentration in the ambient gas. Films prepared by using BaF_2 also require some water to hydrolyze the fluoride (94). Finally, chemical reaction between the superconductor and the substrate during annealing must be limited to prevent contamination of the film or changes in stoichiometry by interdiffusion. To date, a variety of film-forming techniques have been tried in an attempt to satisfy these requirements, but none yet solve all of these problems satisfactorily.

Evaporation. One of the most direct techniques for making films is simply to evaporate the constituents in vacuum and let them condense on an appropriate substrate. Much of the work has been based on coevaporating the metallic elements (15, 89–93) or Cu and Y together with BaF_2 (94, 95) in the presence of a modest pressure of oxygen, usually supplied from a jet directed at the substrate during deposition, to encourage formation of the oxides. If a heated substrate is used, the superconducting phase can be formed in situ (93, 96), but the highest transition temperatures are usually obtained by subsequent annealing in an atmospheric pressure oxygen ambient. This is necessary because the equilibrium pressure of oxygen above the superconductor is about 0.2 torr, much higher than the practical operating pressure of most evaporation systems. A variation of this process is to evaporate layers of the elements (97) or their oxides (98) and then form the compound by interdiffusion during the annealing process.

Most of these techniques can produce films with the onset of superconductivity at temperatures near or above 90 K, but often zero resistance is reached only at a much lower temperature, presumably because of impurity phases forming at grain boundaries. The grain boundary problems can be minimized by using a lattice-matched substrate to produce epitaxial or strongly textured films. Early work showed that single crystal SrTiO_3 was such a substrate (89). In addition, SrTiO_3 has minimal interdiffusion with the superconductor. Zero resistance T_c 's above 90 K on SrTiO_3 are easily obtained and J_c 's from 10^5 A/cm^2 (89) to above 10^6 A/cm^2 (90, 94) at 77 K have been reported. Crystalline films can be formed in situ by heating the substrate to 500° to 700°C during evaporation. Post-deposition annealing in oxygen at a similar temperature results in films with J_c of nearly $4 \times 10^6 \text{ A/cm}^2$ at 77 K (15). Lowering processing temperatures will be crucial to compatibility with semiconductor processing techniques.

Although interesting for basic research, SrTiO_3 is an expensive material with undesirable dc and rf dielectric properties that render it useless for most practical applications. Much of the recent work is directed toward finding alternative substrates or suitable barrier materials to use between the superconductor and more conventional substrates like semiconductors. To date, evaporated films on polycrystalline MgO and ZrO_2 have been made with zero resistance near 90 K, and deposited ZrO_x have had some success as a barrier material on Si, SiO_2 , and Al_2O_3 giving T_c 's above 80 K (95, 99, 100). Because these substrates tend not to produce epitaxial films, the J_c 's are usually much lower ($\approx 10^4 \text{ A/cm}^2$) than on SrTiO_3 and a new approach to the problem may be necessary to get high-quality films with high critical currents on a variety of useful substrates. The recent success in making epitaxial films with $J_c > 4 \times 10^6 \text{ A/cm}^2$ on MgO by sputtering offers hope that this problem may have a solution (16).

Sputtering. The other standard thin-film vacuum-deposition tech-

AS-SINTERED ($J_c = 400 \text{ A/cm}^2$)

MELT-TEXTURED ($J_c = 17000 \text{ A/cm}^2$)

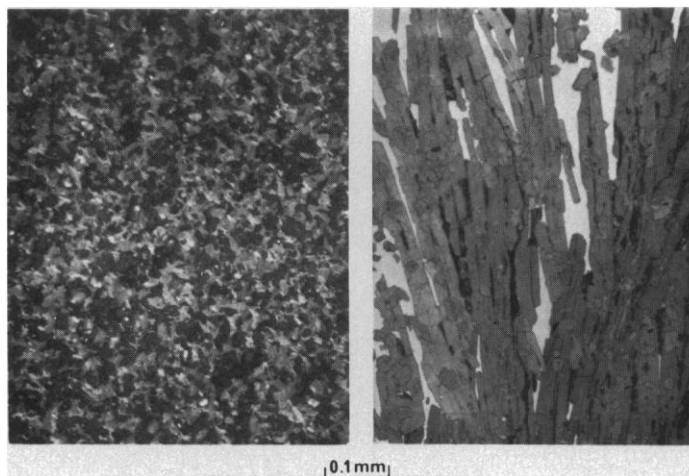


Fig. 8. A comparison of the microstructure and critical current densities of as-sintered (left) and MTG (right) $\text{Ba}_2\text{YCu}_3\text{O}_7$ (83).

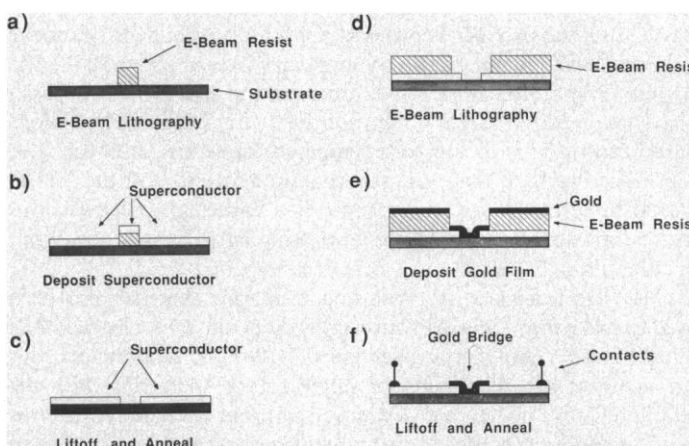


Fig. 9. Schematic of the process for making a superconductor-gold-superconductor microbridge. A resist stencil is formed on the substrate by electron-beam lithography (a), followed by evaporation of the superconductor (b) and liftoff of the resist (c). After annealing the superconductor, the process is repeated to form a gold film bridging the gap between the superconductors (d to f). A final anneal assures good contact between the gold and the superconductor. The device is used by running current between contacts as indicated.

nique is sputtering. This is a well-established commercial practice for other materials, and is a promising candidate for making the perovskite superconductors. As for evaporation, $\text{Ba}_2\text{YCu}_3\text{O}_7$ can be made by cosputtering (101–103) or layering, (104, 105) but the most attractive technique would be sputtering from a single composite target (16, 88, 106–109). In principle, this latter technique offers simplified stoichiometry control and greater uniformity over a large area than deposition from multiple sources. Unfortunately, the different elements in the target have differing sputtering rates and sticking probabilities, necessitating the use of an off-stoichiometric target (16, 106, 110, 111). In such a system, the film stoichiometry changes as the target is consumed, greatly reducing the utility of the process. It is possible to overcome this limitation (110, 111), but the best sputtered films have been made with compensated targets (16). In addition, it is difficult to use single source sputtering as a research tool because each different film composition requires the fabrication of a new target.

Sputtering has demonstrated its potential by producing some of the best films. On SrTiO_3 substrates, single source sputtering of

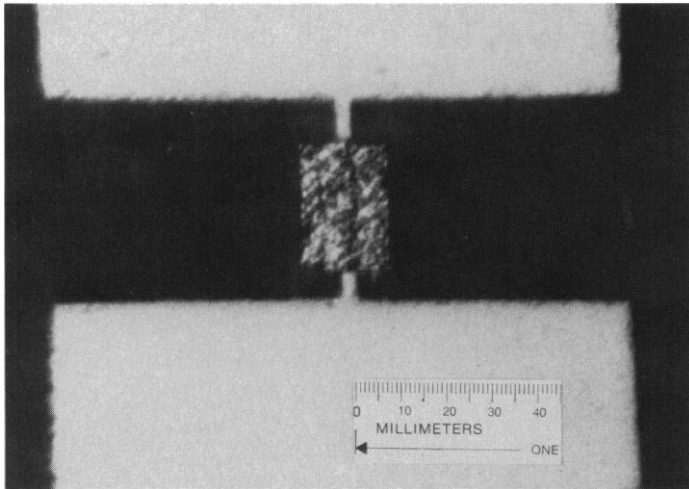


Fig. 10. Micrograph of a completed superconductor-gold-superconductor microbridge. The dimensions are scaled such that 45 mm on the ruler corresponds to 10 μm on the device.

$\text{Ba}_2\text{YCu}_3\text{O}_7$ has produced epitaxial films with current densities above 10^6 A/cm^2 at 77 K and transition temperatures at or above 90 K (88). As with evaporated films, low-temperature in situ growth is possible, even on MgO. High T_c films of the Y, Er, Eu, and Ho analogs have been made with substrate temperatures as low as 650°C (16, 108). The best J_c 's, however, still require a 920°C post-deposition anneal. If composition can be controlled with high precision, this may be an excellent method for fabricating large areas of superconducting films.

Other film techniques. A promising technique that has also been used to make thin films is ablation of a composite target by means of a high-speed, high-energy laser pulse (112–114). In principle, this has many of the advantages of single source sputtering with the additional advantages that deposition without a vacuum system is possible and no specially shaped target is necessary. Films have been made on SrTiO_3 with transition temperatures of about 90 K, usually slightly lower than the starting target material. In principle, the high-speed heating will simplify stoichiometry control by evaporating all elements equally, even though the vapor pressures may differ greatly. In practice, though, there is evidence that the target composition does change because of differential evaporation and more work is needed in this area to understand these effects (115). There is also a problem of obtaining uniform film thickness from a point source evaporation; some combination of multiple-beam ablation and substrate or laser scanning may be necessary.

Another novel technique employs spin-coating of solution or sol-gel precursors on a substrate followed by pyrolysis (116, 117). To date, these materials have reasonable onset temperatures near 90 K and show good epitaxy on SrTiO_3 , but the zero resistance temperatures are less than 80 K, perhaps because the films are not as dense as those produced by other techniques. The low cost and simplicity of this technique makes it worthy of further investigation.

Patterning for thin-film devices. In order to apply thin superconducting films to electronic applications, technologies must be developed to combine them with other materials, like dielectrics or semiconductors, in the intricate patterns required by devices and circuits. A vast array of such techniques have been developed in conjunction with the semiconductor industry (118) and some of these processes are now being investigated for use with the new superconductors. As the tools become available to process these films, a major effort will have to focus on the difficult problems of making the well-controlled structures necessary for electronic devices. The extremely

short coherence length, combined with the highly reactive interfaces, makes implementation of conventional devices difficult.

The most straightforward technique for patterning is simply to coat a superconducting film with a conventional resist material, expose and develop a pattern, and then etch the film. Because of the reactivity of the material, a weak acid is usually sufficient for wet etching, though high-resolution patterns are difficult to obtain because of undercutting of the resist and preferential etching of grain boundaries or second-phase material.

Because of the low resolution and the possibility of moisture damaging the rest of the film, there have been a number of attempts to apply dry etching or patterning techniques to these materials. Reactive ion-beam etching with Cl_2 has been demonstrated as an effective means for removing material (119), and ion implantation can be used to pattern the films by creating normal regions through damage (120). This latter technique has been used to make some of the first thin-film electronic devices in these materials (87).

An alternative dry etching technique that removes all possibility of film damage through reaction with the chemicals used in resist processing is direct laser ablation. Both continuous (121) and pulsed lasers (122, 123) have been used with a demonstrated resolution of a few micrometers. Since it is a direct-write process, it is particularly useful for research applications where flexibility and fast processing of simple patterns is essential.

Rather than etching the superconducting film, it is also possible to form patterns by depositing the film through a photoresist stencil onto the substrate. The resist can be removed with the appropriate solvent, leaving behind the film with a pattern complementary to that in the original resist. The film can then be annealed to form the superconducting phase with the desired pattern. Normally, this process would be difficult because of the highly reactive nature of barium and barium oxide in the pre-annealed film. The use of BaF_2 instead of Ba, though, results in an inert film that is easily processed and can be stored indefinitely without degradation of the properties of the post-annealed material (94, 95). Application of this lift-off process to the fabrication of an electronic device, a superconductor-normal-superconductor microbridge is shown schematically in Fig. 9. Rather than an oxide barrier as in a Josephson tunnel junction, this device consists of a normal metal link between two superconducting films (124). Gold was chosen as the normal metal because it has a long proximity effect coherence length (125) and is known to form good interfaces with $\text{Ba}_2\text{YCu}_3\text{O}_7$ (126, 127). When the bridge is short enough, the normal metal can carry a weak supercurrent by proximity effect. Such devices made with conventional superconductors have a variety of electronic applications including magnetometry and microwave detection. A device with a gold bridge about one micrometer long made by this method is shown in Fig. 10. Preliminary electrical measurements indicate that this device has the microwave and magnetic field behavior expected for a proximity effect microbridge (128). Extending this process to even shorter bridge lengths and better interfaces may lead to high-temperature superconducting devices with practical applications.

Future Prospects

We have attempted to summarize the factors that must be considered in processing the 93 K superconductor $\text{Ba}_2\text{YCu}_3\text{O}_7$ and the current status of those efforts in the two key areas of bulk materials and thin films. Considerable accomplishments have been made in both areas, but major improvements are still needed before any significant practical applications are possible. For bulk materials dramatic improvement in J_c is the major challenge. For thin films the major challenges are transferring technology to practical sub-

strates while maintaining the reproducibility and good superconducting properties (T_c and J_c) demonstrated on SrTiO₃ and MgO.

Most of the processing techniques applicable to thin films are quite different from those of bulk materials. However, a merging of techniques may be beneficial in efforts to obtain high- J_c wire. The eventual use of the new superconductors may require new processing techniques as innovative as the discovery of the materials themselves.

It is not clear at the moment whether Ba₂YCu₃O₇ will be the material of choice for continued development or whether Bi-Sr-Ca-Cu-O or Tl-Ba-Ca-Cu-O with T_c s as high as 110 K and 125 K, respectively, or some other new system will eventually be the most attractive. It is also not clear which processing considerations will be transferable to other systems. Although oxygen processing is critical for Ba₂YCu₃O₇, it appears to be less important for the other systems. However, in (La, Sr)₂CuO₄ the La/Sr ratio is critical. The critical processing parameters for the Bi-Sr-Ca-Cu-O and Tl-Ba-Ca-Cu-O systems remain to be defined but appear to require careful control of crystallographic stacking sequences.

REFERENCES AND NOTES

- J. G. Bednorz and K. A. Müller, *Z. Phys. B* **64**, 189 (1986).
- S. Uchida, H. Takagi, K. Kitzawa, S. Tanaka, *Jpn. J. Appl. Phys.* **26**, L1 (1987).
- K. A. Müller and J. G. Bednorz, *Science* **237**, 1133 (1987).
- M. K. Wu et al., *Phys. Rev. Lett.* **58**, 908 (1987).
- R. J. Cava et al., *ibid.*, p. 1676.
- H. Maeda, Y. Tanaka, M. Fukutomi, T. Asano, *Jpn. J. Appl. Phys. Lett.* **27**, L209 (1988).
- Z. Z. Sheng and A. Herman, *Nature* **332**, 138 (1988).
- C. C. Torardi et al., *Science* **240**, 631 (1988).
- For a general reference on superconductivity, see M. Tinkham, *Introduction to Superconductivity* (Pergamon, Oxford, ed. 2, 1978).
- H. Maletta et al., *Solid State Commun.* **62**, 323 (1987).
- B. Batlogg, A. P. Ramirez, R. J. Cava, R. B. van Dover, E. A. Rietman, *Phys. Rev. B* **35**, 5343 (1987).
- B. Oh et al., *ibid.* **37**, 7861 (1988).
- K. Murata et al., *Jpn. J. Appl. Phys.* **26**, L473 (1987).
- L. F. Schneemeyer, E. M. Gyorgy, J. V. Waszczak, *Phys. Rev. B* **36**, 8804 (1987).
- Y. Bando et al., in *Extended Abstracts of the Topical Meeting on High-Temperature Superconducting Electronic Devices*, June 1988, Miyagi-Zao, Japan (Research and Development Association for Future Electronic Devices, Tokyo, Japan), pp. 11–16.
- H. Itozaki et al., in *ibid.*, pp. 149–156.
- J. D. Hettinger et al., private communication.
- The current densities needed for the applications and performance of Nb-Ti and Nb₃Sn are based on a private communication from E. Occhini.
- Y. Le Page et al., *Phys. Rev. B* **36**, 3617 (1987).
- M. A. Beno et al., *Appl. Phys. Lett.* **50**, 1688 (1987).
- J. J. Capponi et al., *Europhys. Lett.* **3**, 1301 (1987).
- J. E. Greedan, A. H. O'Reilly, C. V. Stager, *Phys. Rev. B* **35**, 8770 (1987).
- F. Beech, S. Miraglia, A. Santoro, R. S. Roth, *ibid.*, p. 8778.
- S. W. Tozer, A. W. Kleinsasser, T. Penney, D. Kaiser, F. Holtzberg, *Phys. Rev. Lett.* **59**, 1768 (1987).
- T. R. Dinger, T. K. Worthington, R. B. Laibowitz, T. R. McGuire, R. J. Gambino, *ibid.* **58**, 2687 (1987).
- C. H. Chen, D. J. Werder, S. H. Liou, J. R. Kwo, M. Hong, *Phys. Rev. B* **35**, 8767 (1987).
- E. A. Hewat, M. Dupuy, A. Bourret, J. J. Capponi, M. Marezio, *Nature* **327**, 400 (1987).
- G. Van Tendeloo, H. W. Zandbergen, S. Amelinckx, *Solid State Commun.* **63**, 389 (1987).
- C. Michel and B. Raveau, *J. Solid State Chem.* **43**, 73 (1982).
- R. S. Roth, J. R. Dennis, K. L. Davis, in *Phase Diagrams for Ceramists Volume VI*, R. S. Roth, J. F. Dennis, H. F. McMurdle, Eds. (American Ceramic Society, Columbus, Ohio, 1987), p. ix.
- K. G. Frase and D. R. Clarke, *Adv. Ceram. Mat.* **2**, 295 (1987).
- G. Wang et al., *ibid.*, p. 313.
- D. W. Murphy et al., *Phys. Rev. Lett.* **58**, 1888 (1987).
- P. H. Hor et al., *ibid.*, p. 1891.
- J. M. Tarascon, W. R. McKinnon, L. H. Greene, G. W. Hull, E. M. Vogel, *Phys. Rev. B* **36**, 226 (1987).
- L. Er-Rakho, C. Michel, J. Provost, B. Raveau, *J. Solid State Chem.* **37**, 151 (1981).
- L. F. Schneemeyer et al., *Nature* **328**, 601 (1987).
- D. L. Kaiser, F. Holtzberg, B. A. Scott, T. R. McGuire, *Appl. Phys. Lett.* **51**, 1040 (1987).
- Y. Hidaka, Y. Enomoto, M. Suzuki, M. Oda, T. Murakami, *J. Crystal Growth* **85**, 851 (1987).
- T. Siegrist et al., *Phys. Rev. B* **36**, 8365 (1987).
- G. Xiao, F. H. Streitz, A. Gavrin, Y. W. Du, C. L. Chien, *ibid.* **35**, 8782 (1987).
- J. M. Tarascon et al., *ibid.* **36**, 8393 (1987).
- Y. K. Tao et al., *J. Mater. Res.* **3**, 248 (1988).
- P. K. Gallagher, H. M. O'Bryan, S. A. Sunshine, D. W. Murphy, *Mat. Res. Bull.* **22**, 995 (1987).
- P. Strobel, J. J. Capponi, C. Chaillout, M. Marezio, J. Tholence, *Nature* **327**, 306 (1987).
- Y. Kubo et al., *Jpn. J. Appl. Phys.* **26**, L768 (1987).
- K. Kishio, J. Shimoyama, T. Hasegawa, K. Kitzawa, K. Fueki, *ibid.*, p. L1228.
- P. K. Gallagher, *Adv. Ceram. Mat.* **2**, 632 (1987).
- A. Santoro et al., *Mat. Res. Bull.* **22**, 1007 (1987).
- J. S. Swinnea and H. Steinfink, *J. Mater. Res.* **2**, 424 (1987).
- D. S. Ginley, P. J. Nigrey, E. L. Venturini, B. Morosin, J. F. Kivak, *ibid.*, p. 733.
- J. van den Berg et al., *Europhys. Lett.* **4**, 737 (1987).
- R. J. Cava et al., *Nature* **329**, 423 (1987).
- J. M. Tarascon et al., in *High Temperature Superconductors, Extended Abstracts of Symposium S, MRS 1987 Spring Meeting*, D. U. Gubser and M. Schluter, Eds. (Materials Research Society, Pittsburgh, PA, 1987), pp. 65–67.
- M. A. Alario-Franco, C. Chaillout, J. J. Capponi, J. Chenavas, *Mat. Res. Bull.* **22**, 1685 (1987).
- C. Chaillout, M. A. Alario-Franco, J. J. Capponi, J. Chenavas, M. Marezio, *Solid State Commun.* **64**, 301 (1987).
- R. M. Fleming et al., *Phys. Rev. B* **37**, 7920 (1988).
- M. Tanaka, M. Terauchi, K. Tsuda, A. Ono, *Jpn. J. Appl. Phys.* **26**, L1237 (1987).
- M. F. Yan et al., *Appl. Phys. Lett.* **51**, 532 (1987).
- R. A. Laudise and R. L. Barns, *ibid.*, p. 1373.
- S. Nakahara et al., *J. Crystal Growth* **85**, 639 (1987).
- M. J. Cima, R. Chiu, W. E. Rhine, in *High-Temperature Superconductors, MRS Symposium Proceedings*, M. B. Brodsky, R. C. Dynes, K. Kitzawa, H. L. Tuller, Eds. (Materials Research Society, Pittsburgh, PA, 1988), vol. 99, pp. 241–244.
- E. C. Behrman et al., *Adv. Ceram. Mat.* **2**, 539 (1987).
- P. Barboux, J. M. Tarascon, L. H. Greene, G. W. Hull, B. G. Bagley, *J. Appl. Phys.* **63**, 2725 (1988).
- D. H. A. Blank, J. Flokstra, G. J. Gerritsma, L. J. M. Van De Klundert, G. J. M. Velders, *Physica B & C* **145**, 222 (1987).
- B. Dunn, C. T. Chu, L.-W. Zhou, J. R. Cooper, G. Gruner, *Adv. Ceram. Mat.* **2**, 343 (1987).
- X. Z. Wang, M. Henry, J. Livage, *Solid State Commun.* **64**, 881 (1987).
- A. R. Moodenbaugh, J. J. Hurst, Jr., R. H. Jones, M. Suenaga, in *High Temperature Superconductors, Extended Abstracts of Symposium S, MRS 1987 Spring Meeting*, D. U. Gubser and M. Schluter, Eds. (Materials Research Society, Pittsburgh, PA, 1987), pp. 100–101.
- M. L. Kaplan and J. J. Hauser, *Mat. Res. Bull.* **23**, 287 (1988).
- S. M. Johnson, M. I. Gusman, D. J. Rowcliffe, T. H. Geballe, J. Z. Sun, *Adv. Ceram. Mat.* **2**, 337 (1987).
- R. D. Poeppel, B. K. Flandermeyer, R. J. Dusek, I. D. Bloom, in *Chemistry of High-Temperature Superconductors*, D. L. Nelson, M. S. Whittingham and T. F. George, Eds. (American Chemical Society, Washington, DC, 1987), pp. 261–265.
- D. W. Johnson, Jr. et al., *Adv. Ceram. Mat.* **2**, 364 (1987).
- S. Jin et al., *Appl. Phys. Lett.* **51**, 855 (1987).
- A. F. Henricksen, paper presented at *Ceramtec '88*, 2 to 3 February, Dearborn, MI (American Society for Metals, International, Metals Park, OH, 1988).
- L. E. Murr, A. W. Hare, N. G. Eror, *Nature* **329**, 37 (1987).
- Filamentary A-15 Superconductors*, M. Suenaga and A. F. Cook, Eds. (Plenum Press, New York, 1980).
- S. Jin, R. C. Sherwood, R. B. van Dover, T. H. Tiefel, D. W. Johnson, Jr., *Appl. Phys. Lett.* **51**, 203 (1987).
- S. Jin, T. H. Tiefel, R. C. Sherwood, G. W. Kammlott, S. M. Zahurak, *ibid.*, p. 943.
- R. Halder, Y. Z. Lu, B. G. Giessen, *ibid.*, p. 538.
- S. Matsuda, M. Okada, T. Morimoto, T. Matsumoto, K. Aihara, in *High-Temperature Superconductors, MRS Symposium Proceedings*, M. B. Brodsky, R. C. Dynes, K. Kitzawa, H. L. Tuller, Eds. (Materials Research Society, Pittsburgh, PA, 1988), vol. 99, pp. 695–698.
- J. W. Ekin, *Adv. Ceram. Mat.* **2**, 586 (1987).
- S. Jin et al., *Phys. Rev. B* **37**, 7850 (1988).
- S. Jin et al., *Appl. Phys. Lett.* **52**, 2074 (1988).
- O. K. Kwon, B. W. Langley, R. F. W. Pease, M. R. Beasley, *IEEE Electron Dev. Lett.* **8**, 582 (1987).
- S. Tewksbury, L. Hornak, M. Hataman, *Superconductivity Theory and Applications* (World Scientific, Singapore, in press).
- J. E. Zimmerman, J. A. Beall, M. W. Cromar, R. H. Ono, *Appl. Phys. Lett.* **51**, 617 (1987).
- R. H. Koch, C. P. Umbach, G. J. Clark, P. Chaudhari, R. B. Laibowitz, *ibid.*, p. 200.
- Y. Enomoto, T. Murakami, M. Suzuki, K. Moriwaki, *Jpn. J. Appl. Phys.* **26**, L1248 (1987).
- P. Chaudhari, R. H. Koch, R. B. Laibowitz, T. R. McGuire, R. J. Gambino, *Phys. Rev. Lett.* **58**, 2684 (1987).
- B. Oh et al., *Appl. Phys. Lett.* **51**, 852 (1987).
- C. Webb et al., *ibid.*, p. 1191.
- J. Kwo et al., *Phys. Rev. B* **36**, 4039 (1987).
- D. K. Lathrop, S. E. Russek, R. A. Burhman, *Appl. Phys. Lett.* **51**, 1554 (1987).
- P. M. Mankiwich et al., *ibid.*, p. 1753.
- P. M. Mankiwich et al., in *High-Temperature Superconductors, MRS Symposium Proceedings*, M. B. Brodsky, R. C. Dynes, K. Kitzawa, H. L. Tuller, Eds. (Materials Research Society, Pittsburgh, PA, 1988), vol. 99, pp. 119–125.
- T. Terashima, K. Iijima, K. Yamamoto, Y. Bando, H. Mazaki, *Jpn. J. Appl. Phys.*

- 27, L91 (1988).
97. B-Y. Tsauro, M. S. Dilorio, A. J. Strauss, *Appl. Phys. Lett.* **51**, 858 (1987).
 98. Z. L. Bao *et al.*, *ibid.*, p. 946.
 99. M. Naito *et al.*, *J. Materials Res.* **2**, 713 (1987).
 100. A. Mogro-Campero, L. G. Turner, *Appl. Phys. Lett.* **52**, 1185 (1988).
 101. K. Char, A. D. Kent, A. Kapitulnik, M. R. Beasley, T. H. Geballe, *ibid.* **51**, 1370 (1987).
 102. M. Scheuermann *et al.*, *ibid.*, p. 1951.
 103. R. E. Somekh *et al.*, *Nature* **326**, 857 (1987).
 104. R. M. Silver, J. Talvacchio, A. L. deLozanne, *Appl. Phys. Lett.* **51**, 2149 (1987).
 105. T. Aida, T. Fukazawa, K. Takagi, K. Miyauchi, *Jpn. J. Appl. Phys.* **26**, L1489 (1987).
 106. J. L. Makous *et al.*, *Appl. Phys. Lett.* **51**, 2164 (1987).
 107. M. Hong, S. H. Liou, J. Kwo, B. A. Davidson, *ibid.*, p. 694.
 108. H. Adachi, K. Hirochi, K. Setsune, M. Kitabatake, K. Wasa, *ibid.*, p. 2263.
 109. H. Asano, K. Tanabe, Y. Katoh, S. Kubo, O. Michikami, *Jpn. J. Appl. Phys.* **26**, L1221 (1987).
 110. H. C. Li, G. Linker, F. Ratzel, R. Smithy, G. Geerk, *Appl. Phys. Lett.* **52**, 1098 (1988).
 111. G. K. Wehner, Y. H. Kim, D. H. Kim, A. M. Goldman, *ibid.*, p. 1187.
 112. D. Dijkkamp *et al.*, *ibid.* **51**, 619 (1987).
 113. J. Narayan, N. Biunno, R. Singh, O. W. Holland, O. Auciello, *ibid.*, p. 1845.
 114. A. M. DeSantolo, M. L. Mandich, M. F. Jarrold, J. E. Bower, S. Sunshine, in *Thin Film Processing and Characterization of High Temperature Superconductors*, AIP Conference Proceedings No. 165, J. Harper, R. Colton, and L. Feldman, Eds. (American Institute of Physics, New York, 1988), pp. 174–181.
 115. O. Auciello, A. R. Krauss, J. Santiago-Aviles, A. F. Schreiner, D. M. Gruen, *Appl. Phys. Lett.* **52**, 239 (1987).
 116. C. E. Rice, R. B. VanDover, G. J. Fisanick, *ibid.* **51**, 1842 (1987).
 117. M. E. Gross, M. Hong, S. H. Liou, P. K. Gallagher, J. Kwo, *ibid.* **52**, 160 (1988).
 118. S. M. Sze, Ed., *VLSI Technology*, (McGraw-Hill, New York, 1983).
 119. S. Matsui, N. Takado, H. Tsuge, K. Asakawa, *Appl. Phys. Lett.* **52**, 69 (1988).
 120. G. J. Clark, F. K. LeGoues, A. D. Marwick, R. B. Laibowitz, R. Koch, *ibid.* **51**, 1462 (1988).
 121. G. J. Fisanick *et al.*, in *Thin Film Processing and Characterization of High Temperature Superconductors*, AIP Conference Proceedings No. 165, J. Harper, R. Colton, L. Feldman, Eds. (American Institute of Physics, New York, 1988), pp. 189–196.
 122. A. Inam *et al.*, *Appl. Phys. Lett.* **51**, 1112 (1987).
 123. M. Scheuermann *et al.*, *ibid.*, p. 1951.
 124. T. Van Duzer and C. W. Turner, *Principles of Superconductive Devices and Circuits* (Elsevier, New York, 1981).
 125. R. B. VanDover, A. De Lozanne, R. E. Howard, W. L. McLean, M. R. Beasley, *Appl. Phys. Lett.* **37**, 838 (1980).
 126. A. D. Wieck, *ibid.* **52**, 1017 (1988).
 127. J. W. Ekin *et al.*, *ibid.*, p. 1819.
 128. P. M. Mankiwich *et al.*, in *Extended Abstracts of the Topical Meeting on High-Temperature Superconducting Electronic Devices*, June 1988, Miyagi-Zao, Japan (Research and Development Association for Future Electronic Devices, Tokyo, Japan), pp. 157–160.
 129. We thank all of our colleagues at AT&T Bell Laboratories for continued collaborations and valuable discussions. We especially thank J. Thomson, D. Lishner, and R. Stanton for preparation of the screen-printed materials and W. W. Rhodes for the tape-cast material, and P. M. Mankiwich for helpful suggestions to this paper. We also thank our scientific colleagues over the world for sharing their preprints with us.

Synthesis of Buried Oxide and Silicide Layers with Ion Beams

ALICE E. WHITE AND K. T. SHORT

Ion implantation, because it is inherently a strongly nonequilibrium process, can add a new dimension to materials studies. A large variety of chemical elements may be readily introduced into a target substrate by ion bombardment at concentrations considerably greater than the normal solid solubilities. In addition, the interaction of the accelerated ions with the target produces lattice defects. Both effects have been studied extensively in experiments directed at understanding the mechanisms of formation of buried oxide and silicide layers in silicon with high-dose ion implantation. These layers have properties that are difficult to attain with conventional techniques.

EXPERIMENTS IN ION IMPLANTATION WERE FIRST PERFORMED almost 40 years ago by nuclear physicists (1). More recently, ion implanters have become permanent fixtures on the processing lines of integrated circuits. Manufacture of the more complex chips may involve as many as ten different ion implantation steps. Implantation is used primarily at fluences of 10^{12} to 10^{13} ions/cm² to tailor the electrical properties of a semiconductor substrate. Figure 1A shows a cross-sectional view of a typical complementary metal-oxide-semiconductor (CMOS) device structure consisting of both *n*- and *p*-channel MOSFETs (MOS field effect transistors) (2, 3). Other conventional uses of implantation in semiconductors include amorphization for isolation [particularly in

gallium arsenide (GaAs) circuits] (4) and for fundamental solid-state studies (5) and mixing of multilayer films for phase formation (6). Implantation of nitrogen into metals has been used since the early 1970s to improve the corrosion and wear resistance of base metals such as steel (7) and has been exploited in the manufacture of bearings, artificial joints, and stamping punches and dies. In the past, applications of implantation were limited by the small beam currents that were available, but recently a new generation of high-current implanters has entered the market. This high current capability allows us to implant the extremely large concentrations required for our work on compound synthesis—in some cases five orders of magnitude higher than those required for doping.

The small fluences required by most conventional applications of implantation represent an almost negligible perturbation in the composition of the target (<1 atomic %). In general, the concentrations of implanted ions are so small that they are hard to detect directly with most analysis techniques, and the damage to the crystalline lattice may be used as the earmark of the implant. In this article, we consider implantation that significantly alters the composition of the target, specifically implantation of enough ions to create a compound. Typical solids have densities of $\sim 5 \times 10^{22}$ atoms/cm³, so formation of a compound AB, where B is the substrate material, would require a fluence of $\sim 2.5 \times 10^{17}$ ions/cm² for a 1000-Å layer. If the doping implantations take about 1 min to complete, these implantations would take 2 months at the usual implanter beam current. Higher currents are therefore essential.

The authors are at AT&T Bell Laboratories, Murray Hill, NJ 07974.